

## EARLY DETECTION OF BIOTERRORISM: MONITORING DISEASE USING AN AGENT-BASED MODEL

Summer (Xia) Hu

Sean Barnes  
Bruce Golden

Department of Mathematics  
University of Maryland  
College Park, MD 20742, USA

Robert H. Smith School of Business  
University of Maryland  
College Park, MD 20742, USA

### ABSTRACT

We propose an agent-based model to capture the transmission patterns of diseases caused by bioterrorism attacks or epidemic outbreaks and to differentiate between these two scenarios. Focusing on a region of three cities, we want to detect a bioterrorism attack before a sizeable proportion of the population is infected. Our results indicate that the aggregated infection and death curves in the region can serve as indicators in distinguishing between the two disease scenarios: the slope of the epidemic infection curve will increase initially and decrease afterwards, whereas the slope of the bioterrorism infection curve will strictly decrease. We also conclude that for a bioterrorism outbreak, the bioterrorism source city becomes more dominant as the local working probability  $p_L$  increases. In contrast, the behavior of individual cities for the epidemic model presents a “time-lag” pattern, especially when  $p_L$  is large. As  $p_L$  decreases, the individual city’s dynamic curves converge as time progresses.

### 1 INTRODUCTION

Bioterrorism, namely the intentional release of viruses, bacteria, or other toxic biological agents, is considered a significant threat to the United States. Early detection of a potential bioterrorism incident is vital for controlling diseases and limiting the damage. However, as some candidate bioterrorism diseases (e.g., anthrax and viral hemorrhagic fever) present symptoms in humans similar to those of common illnesses (e.g., the flu), it is difficult to quickly distinguish between a bioterrorism outbreak and a natural disease. The existing techniques for early detection have failed to differentiate between epidemic diseases and bioterrorism attacks, required too many assumptions, or seemed too complex.

Wagner et al. (2001) summarized mathematical foundations of early detection and reviewed previous work concerning the measurement of detection timelines. Using signal detection theory and decision theory, the authors identified strategies to improve the timeliness of detection and position ongoing detection system development within that framework. Lober et al. (2002) discussed six existing public health surveillance systems, which were designed to enhance early detection of bioterrorism events. However, their method cannot distinguish between a bioterrorism outbreak and a natural disease.

Yahav et al. (2013) proposed a conceptual framework for differentiating between bioterrorism and epidemic scenarios. They constructed a multilayered network that included social and spatial components, and incorporated functional principal components analysis (fPCA) to characterize disease transmission. Despite the accurate results from their method, its shortcoming is that the model contains many arbitrary assumptions about the structure of the social, location, and human-location networks.

Our goal is to propose a method that is both accurate and easy to implement in practice. In this paper, we develop a simple-structured, agent-based model to capture the transmission patterns of diseases caused by bioterrorism attacks or epidemic outbreaks. Based on the aggregated regional infection trends or the

individual infection curves at each city, our research seeks to detect an attack when only a small proportion of the population is infected.

In Section 2, we discuss our methodology and simulation models for the bioterrorism and epidemic outbreaks, where human behaviors are based upon travel patterns during the day and at night. In Section 3, we present results for both models under various local working probabilities and validate our simulation results with a two-phase mathematical model for the epidemic case. In Section 4, we include some conclusions and a mention of future work. We are particularly interested in distinguishing between these two disease scenarios when the first outbreak time is uncertain and in identifying appropriate infection control measures.

## **2 METHODOLOGY**

We conduct experiments in computer-generated households and work places at three cities within a region, and simulate the spread of disease via bioterrorism and epidemic scenarios, respectively. The experiments are implemented using NetLogo (v. 5.0.4), an agent-based programming language and integrated modeling environment (Wilensky 1999). Our primary assumption is that the epidemic disease is transmitted only via human interactions (Clayton, Hills, and Pickles 1993), whereas bioterrorism is transmitted only through a person's proximity to the source of the attack (CDC 2007).

### **2.1 General Model Description**

Our preliminary results are based on 900 households in three connected cities—A, B, and C. We constrain the environment to be closed: no immigrants from the outside and no newborns from within the three cities. The models for the epidemic disease and the bioterrorism attack share a few common assumptions. We describe their shared properties in this section, and discuss their unique assumptions in Sections 2.2 and 2.3.

There are two phases to each model—SETUP and GO. In the SETUP phase, three square-shaped cities are generated. Our initial experiments suggest that city size does not matter as long as we analyze the proportion infected and dead, rather than the absolute counts. Therefore, we can assume all the cities are the same size, and generate 300 households per city. We also assume that the number of residents in each household is drawn randomly from the following distribution: [1 2 2 3 3 4 4 5 5 6]. In the GO phase, the model will oscillate between a daytime state (6 a.m. – 6 p.m.) and a nighttime state (6 p.m. – 6 a.m.). We assume that only public interactions take place during the daytime state and only within-household interactions take place during the nighttime state. Figure 1 demonstrates our model description in an activity-flow diagram.

We suppose that each person's work city is fixed throughout the simulation. During the daytime state, some people work from their home city with a predefined local working probability  $p_L$ , whereas the remaining people travel to the other two cities for work with an equal chance. We make this assumption because for most people, their work or school cities are usually fixed. In addition, we assume that each person's destination inside the travel city follows a bivariate normal distribution, which is not fixed from day to day. This is based on the general observation that most cities have a central area where many people work, and a person might appear in various locations within the city for different purposes. Figure 2 demonstrates the initial uniformly distributed spread of households and the bivariate normally distributed travel destinations.

In each model, we assign one of four states to each person: healthy, infected, recovered (and immune), and dead. We assume everyone in the model must be in one of these states, and initially no one is immune to the disease. This is because if we assume a percentage of residents are immune to the disease at the initial state, then the infection curves will shrink by approximately that percentage in height (see the Appendix for a more detailed justification). We assign an infection radius  $R$  for each disease, indicating the immediate area within which the disease is transmissible.

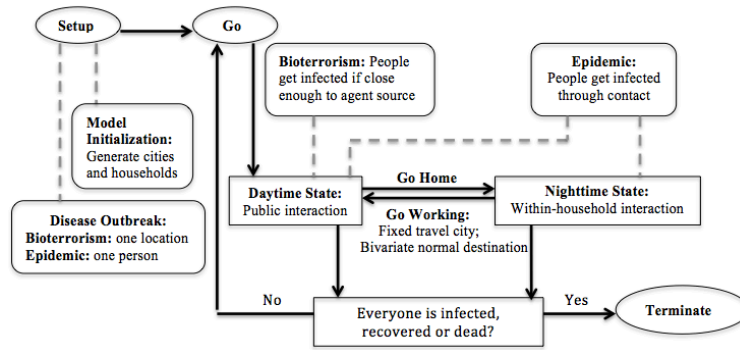


Figure 1: Activity-flow diagram, where ovals represent the model phase and arrows indicate the flow of progress. Rounded rectangles connected to the dashed lines explain the process in ovals and rectangles.

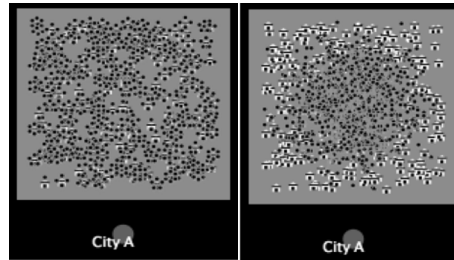


Figure 2: Initial setup for uniformly distributed households and bivariate normally distributed work locations in city A. The black and white house-shapes stand for households, and the grey circles with a black dot in the center represent people.

In our model, each infected individual has a predetermined chance of death or recovery. We assume those who will die pass away after a specific amount of time (i.e., death survival time) and those who will recover will do so by the end of some stochastic recovery time  $t_R$ . The above assumption is based on the observation that if an infected individual dies, he tends to die quickly, and if he survives, the recovery usually takes much longer. If we denote the average recovery time for a disease to be  $\bar{t}$ , then we assume the recovery time  $t_R$  is drawn from a truncated normal distribution  $N(\bar{t}, \sqrt{\bar{t}/6})$ , where  $t_R = 2\bar{t}$  if  $t_R > 2\bar{t}$  and  $t_R = 3$  if  $t_R$  is negative for the epidemic case, and  $t_R = 3\bar{t}$  if  $t_R > 3\bar{t}$  and  $t_R = 8$  if  $t_R$  is negative for the bioterrorism case (Guillemin 1999, Atkinson et al. 2005).

There are a few variables in our models; however, most of their values are predetermined and can be drawn from historical data (e.g., recovery probability, average recovery time). For parameters whose values are uncertain (e.g., home/work infection probability, infection radius), we try to assign values that are as reasonable as possible or we deliberately control the infection dynamics of the epidemic and bioterrorism cases to be similar, so as to ensure that we can distinguish these two cases even for the most difficult situations.

There are three diseases in our experiment: normal epidemic, extreme epidemic, and bioterrorism disease, where the normal and extreme epidemic share the same simulation model yet differ in their recovery probability. An example of an extreme epidemic would be a super influenza pandemic, such as the catastrophic 1918 pandemic, which had an extremely high death rate (Patterson and Pyle 1991, Taubenberger and Morens 2006).

## 2.2 Bioterrorism Model

We propose a conceptual model for a bioterrorism disease. We assume the disease breaks out in one city (e.g., city C in our case). It only transmits to people who are within a certain distance from the source, and does not transmit among humans. During the daytime, a person may get infected (if near the source), recover, or die. During the nighttime, people go home, where no disease transmission occurs. We utilize a maximum location infection probability  $p_M$  to represent the probability of a person being infected near the bioterrorism source. For a healthy person who is within the infection radius  $R$  of a bioterrorism source, the probability of getting infected in the source city is inversely proportional to the square of the distance from the source location.

We assume the bioterrorism source is located at the city center, where the population density is highest. This is because the goal of bioterrorists is to create as much chaos as possible; thus, the city center would be an ideal attack location. Because bioterrorism has a high mortality rate—ranging from 0.2 to 0.9 if untreated, and 0.01 to 0.45 if treated in time, we set the death probability to be 0.7 without distinguishing whether the patient is being treated or not (Bravata et al. 2006, CIDRAP 2013). We also assume  $p_M$  is high (0.6). This is based on the properties of most biological agents (FAS 2014). Finally, we assign survival times and average recovery times drawn from practice (Guillemin 1999, Atkinson et al. 2005). A complete listing of parameter settings of the bioterrorism model is shown in Table 1. Later in Section 3.2, we will consider many combinations of parameter settings and develop the maximum, minimum, and median dynamic curves.

Table 1: Parameter Setup – Bioterrorism.

| Parameter                                    | Value (s)        |
|--|------------------|
| Average Recovery Time $\bar{t}$              | 15 days          |
| Death Survival time $t_D$                    | 3 days           |
| Local Working Probability $p_L$              | 0.33, 0.6, 0.9   |
| Recovery Probability $p_R$                   | 0.3              |
| Death Probability                            | 0.7              |
| Maximum Location Infection Probability $p_M$ | 0.6              |
| Infection Radius $R$                         | 10               |
| Outbreak Location                            | Center of city C |

## 2.3 Epidemic Model

We assume the epidemic initiates with a single person, and the disease propagates to other individuals within the region through human interaction only. During the daytime, people within the influence radius  $R$  of an infected person will acquire the flu with a work infection probability  $p_W$ . During the nighttime, only people who live with an infected family member will get infected, with a home infection probability  $p_H$ . In both cases, a patient may recover or die from the disease.

We assume the work infection probability  $p_W$  is low (0.03), and the home infection probability  $p_H$  is relatively high (0.4), due to the intimacy among family members. We apply 0.001 and 0.3 as the death probability for normal flu and super influenza, respectively (Patterson and Pyle 1991; Taubenberger and Morens 2006; Knobler et al. 2005). The parameter settings are presented in Table 2.

Table 2: Parameter Setup – Normal & Extreme Epidemic.

| Parameter                        | Value (s)                                 |
|----------------------------------|---|
| Average Recovery Time $\bar{t}$  | 10 days                                   |
| Death Survival Time $t_D$        | 5 days                                    |
| Local Working Probability $p_L$  | 0.33, 0.6, 0.9                            |
| Recovery Probability $p_R$       | 0.999 for normal flu, 0.7 for extreme flu |
| Death Probability                | 0.001 for normal flu, 0.3 for extreme flu |
| Infection Radius $R$             | 3   |
| Work Infection Probability $p_W$ | 0.03                                      |
| Home Infection Probability $p_H$ | 0.4                                       |
| Initial Infection Number         | 1   |

### 3 RESULTS

Our results are based on the interaction between three cities, because this configuration is representative of many metropolitan areas. In this experiment, we only consider the initial 15 days. This is partially due to the uninhibited environment of the initial spread of a disease (i.e., no residential protection like mask-wearing and improved hygiene, and no human intervention like quarantine, travel restrictions or vaccination). In addition, we are only interested in quickly distinguishing bioterrorism from an epidemic in an early stage, so the study of the spread during the initial days is reasonable.

In the following experiments, we vary the local working probability  $p_L$  from 0.9 to 0.33, due to the belief that many residents will work locally, but there is still interaction among cities. Experiments indicate that our model has low variance across many replications, therefore we base our results on the mean outcome under the same parameter settings. In Figure 3, we see the aggregated infection curves over three cities for our three scenarios when the local working probability  $p_L = 0.6$ . We observe that the normal and extreme epidemics share the similar “S” curve, whereas the bioterrorism curve has a curve with a strictly decreasing slope. However, in practice, when the initial outbreak time is unknown, it is difficult to tell whether an unknown disease is a bioterrorism outbreak from day 2 to day 6 or an epidemic disease from day 5 to day 10.

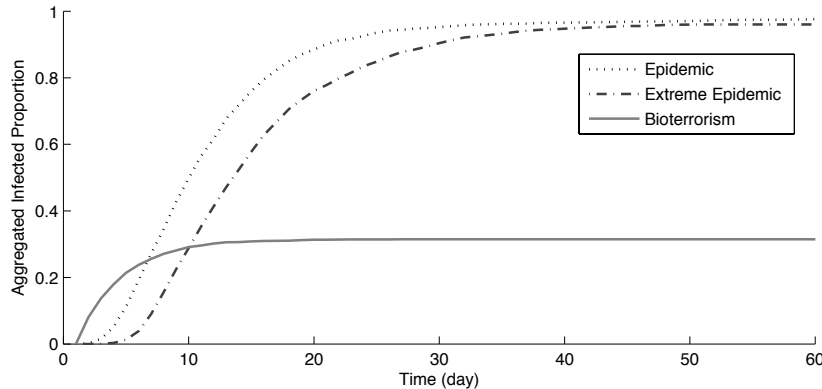


Figure 3: Comparison between the aggregated infection curves of three diseases among three cities when local working probability  $p_L = 0.6$ .

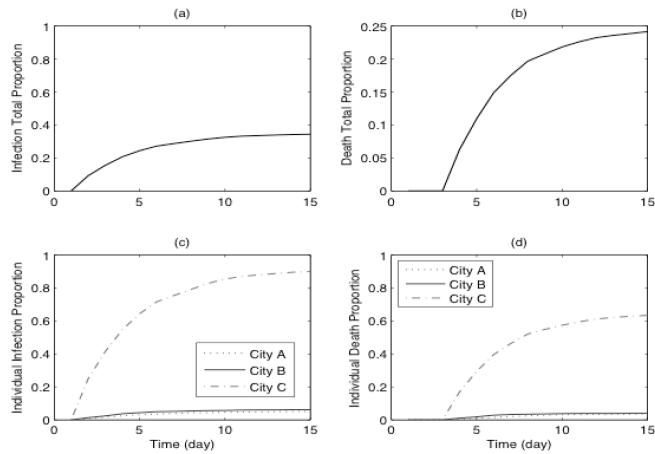


Figure 4: Aggregated infection (a) and death (b) curves and individual city infection (c) and death (d) curves in bioterrorism model for  $p_L = 0.9$ .

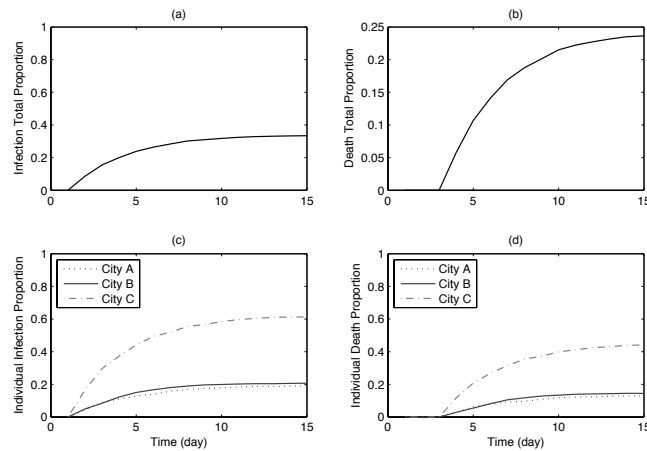


Figure 5: Aggregated infection (a) and death (b) curves and individual city infection (c) and death (d) curves in bioterrorism model for  $p_L = 0.6$ .

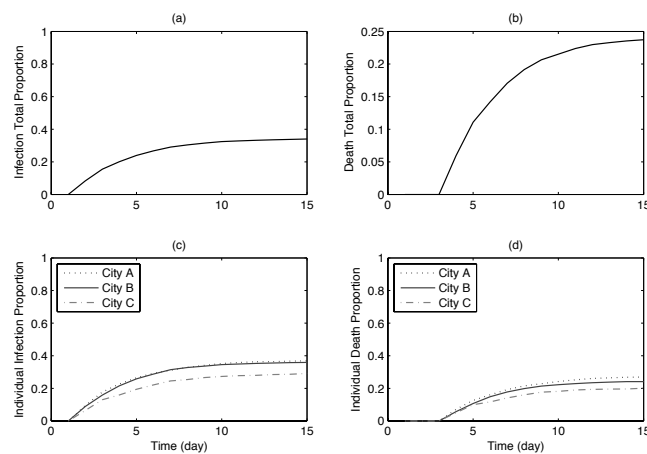


Figure 6: Aggregated infection (a) and death (b) curves and individual city infection (c) and death (d) curves in bioterrorism model for  $p_L = 0.33$ .

### 3.1 Bioterrorism Scenario

In the following analysis, we gradually decrease  $p_L$  from 0.9 to 0.33 while keeping the other parameters fixed. Experiments indicate that a high  $p_L$  is not always associated with high proportions of aggregated infection and death. The bioterrorism curves share an increasing trend with a decreasing slope, which is due to the shrinking susceptible pool of population that travel to the source location.

Figures 4, 5, and 6 present aggregated and individual city infection and death curves for local working probability  $p_L$  equal to 0.9, 0.6, and 0.33. As  $p_L$  decreases from 0.9 to 0.33, the overall mobility of the population increases, yet the aggregated infection and death proportion among the three cities does not vary much. However, the infection curves for individual cities present distinct characteristics. When  $p_L$  is 0.9, the infection curve for the bioterrorism source city C dominates the others, with a city infection proportion of 0.9, whereas the infection proportion for the other two cities is less than 0.1. As  $p_L$  decreases to 0.6, city C's infection proportion decreases to 0.6, while the infection proportion of the other two cities increases to 0.2. When  $p_L$  is 0.33, the three cities have a similar infection proportion at 0.33, and the difference among the three city curves is indistinguishable. The decrease in infection dominance of city C is a result of our fixed work city assumption. When  $p_L$  is high, few people from the other two cities have the chance to approach the bioterrorism source in city C, thus a very small portion of people from cities A and B can get infected. Therefore,  $p_L$  has little to do with the overall infection or death proportion among the three cities. However, as  $p_L$  decreases and, thus, the mobility of the population increases, the three cities have similar infection and death curves.

### 3.2 Epidemic Scenario

We apply a similar method to study epidemic disease transmission. A normal flu epidemic differs from an extreme epidemic only in death rates, so here we only present the extreme epidemic curve, for it demonstrates a more severe death curve. Experiments indicate that the infection and death proportion curves in the extreme epidemic model for various  $p_L$  share a similar “S” shape, which is due to the increasing infection agents at the beginning stage and a shrinking susceptible pool later on.

Figures 7, 8, and 9 present aggregated and individual city death and infection curves for  $p_L = 0.9, 0.6,$  and  $0.33,$  respectively. In contrast to the bioterrorism case, the behavior of individual cities is relatively close, but the transmission curves present a “time-lag” pattern, especially when  $p_L$  is large. For example, when  $p_L = 0.9,$  the infection curve of the source city (C) starts to grow sooner. Yet after about two days, the infection curves of city A and city B begin to grow in the same manner. Such a phenomenon is the result of the epidemic transmission property—each person can be considered as a “disease source”, thus once a non-initial-outbreak city has an infected person, this city will reproduce the disease dynamics of the initial outbreak city, given that they have similar transmission characteristics. As  $p_L$  decreases, the difference between the initial outbreak city and the other two cities becomes less visible.

### 3.3 Model Validation

In this section, we propose a two-phase equation-based model to validate our epidemic simulation results. We retain the simulation model assumptions such as the population details, immunity levels and travel patterns, and let  $S(t), I(t)$  and  $R(t)$  represent the susceptible, infected, and recovered population in the three cities at time  $t$ . For the epidemic scenario, we adopt a modified discrete version of the Kermack-McKendrick SIR model (Mahaffy and Dockery 2013):

$$S_{t+1} = S_t - \frac{\theta S_t I_t}{N}, \quad I_{t+1} = I_t + \frac{\theta S_t I_t}{N} - \gamma I_t, \quad \text{and} \quad R_{t+1} = R_t + \gamma I_t,$$

where  $\theta = \alpha\beta$ , with  $\alpha$  representing the average number of contacts per individual per unit time and  $\beta$  representing the transmission probability during each contact, and the recovery rate  $\gamma = [\bar{\tau} + (1 -$

$p_R)t_D]^{-1}$ . We assume the model oscillates between the day and night phases. Accordingly,  $N$  stands for the population at a household in the night phase ( $N_H$ ) and the population of a city in the day phase ( $N_C$ ).

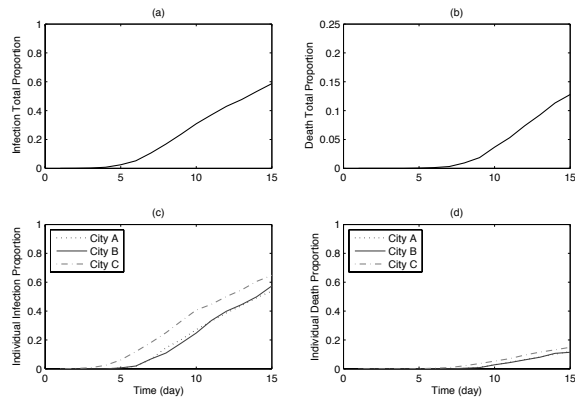


Figure 7: Aggregated infection (a) and death (b) curves and individual city infection (c) and death (d) curves in the extreme epidemic model for  $p_L = 0.9$ .

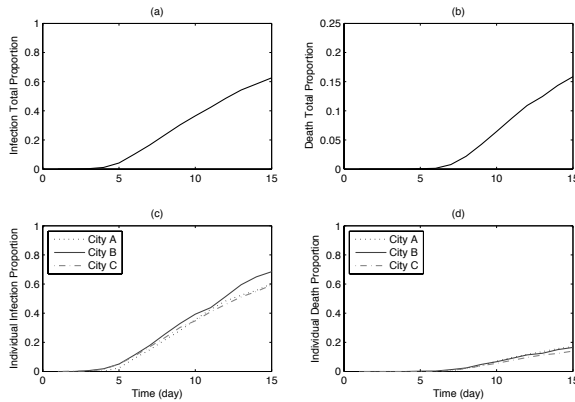


Figure 8: Aggregated infection (a) and death (b) curves and individual infection (c) and death (d) curves in the extreme epidemic model for  $p_L = 0.6$ .

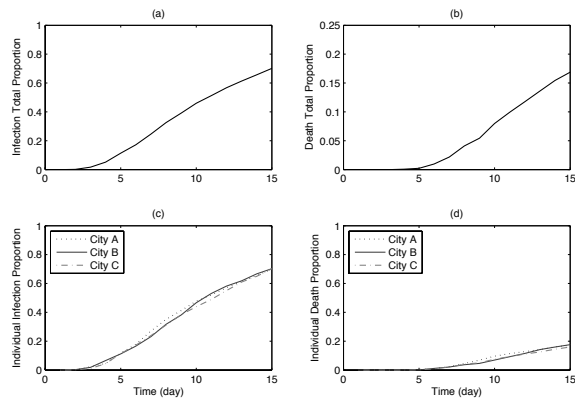


Figure 9: Aggregated infection (a) and death (b) curves and individual city infection (c) and death (d) curves in the extreme epidemic model for  $p_L = 0.33$ .

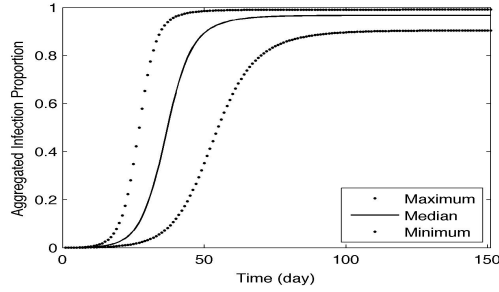


Figure 10: Aggregated infection curves for the epidemic disease from an equation-based model. The maximum, median, and minimum curves are based on experiments with the home infection probability  $p_H$  as it ranges from 0.1 to 0.7 and the work infection probability  $p_W$  as it ranges from 0.01 to 0.08.

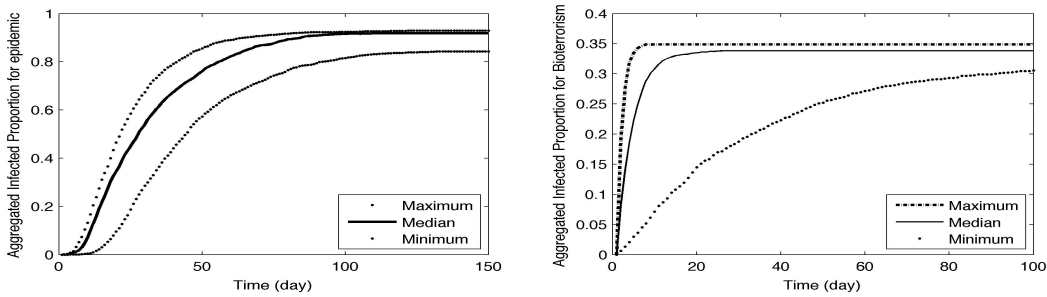


Figure 11: Aggregated infection curves for the epidemic (left) and bioterrorism (right) scenarios from our simulation model, with  $p_L$  ranging from 0.1 to 0.9. In the epidemic case, the home infection probability  $p_H$  ranges from 0.1 to 0.7 and the work infection probability  $p_W$  ranges from 0.01 to 0.08. In the bioterrorism case, the infection range  $R$  changes from 3 to 15, while the maximum location infection probability  $p_M$  changes from 0.5 to 0.9.

We apply the home and work infection formula:  $\theta_H = (N_H - 1) \cdot P_H$  and  $\theta_w = P_w \cdot R/r \cdot N_C$ , where  $r$  stands for the city radius. Figure 10 shows the aggregated infection curves for this two-phase equation-based model.

In comparison, transmission curves generated from our simulation model (Figure 11, left) exhibit a similar shape as the two-phase SIR model for the epidemic case, and with a much shorter model running time. In addition, our agent-based model can keep track of each individual’s behavior, whereas the mathematical model fails to distinguish between individuals and their travel patterns. Since analytical bioterrorism models that characterize infection dynamics, location, and transportation are not available yet (Roberts 2003), we are not able to validate our bioterrorism model using a similar approach. However, our simulation results for both epidemic and bioterrorism diseases resemble the transmission curve shapes produced by the model of Yahav et al., which are generated over a complex social and location network.

## 4 CONCLUSION AND FUTURE RESEARCH

### 4.1 Next Steps

We proposed two models with simple structures and relatively few assumptions to capture the essence of bioterrorism and epidemic transmission. Our models indicate that the aggregated infection and death curves for a region can serve as indicators in differentiating the two scenarios: the slope of the epidemic infection curve will increase initially and decrease afterwards, whereas the slope of the bioterrorism

infection curve will strictly decrease. Our results also show that the local working probability  $p_L$  has little to do with the aggregated infection proportion for both scenarios; yet for the bioterrorism outbreak, as  $p_L$  increases, the bioterrorism source city exhibits a more dominant infection proportion. In contrast, for the epidemic model, the behavior of individual cities presents a “time-lag” pattern, especially when  $p_L$  is large. As  $p_L$  decreases, the three dynamic curves (one for each city) converge as time progresses.

We are particularly interested in distinguishing between the two scenarios when the first outbreak time is not known. In practice, due to the time delay of reporting and seasonal noise, we may not be aware of the disease outbreak until after numerous cases or deaths, and it would be difficult to trace back and determine the first occurrence time. Because bioterrorism and epidemic diseases present similar transmission dynamics curves in their initial occurrence, the question becomes how to discriminate the two scenarios given an unknown first outbreak time. For example, in Figure 2, it is obvious that the dynamics of the bioterrorism outbreak and epidemic disease are different; however, if we simply observe an overall infection curve with an increasing shape, how can we tell whether a disease is at the initial stage of a bioterrorism outbreak or in an ongoing process of an epidemic disease? We want to develop tests to quantify such differences.

In future work, we will develop measures to distinguish the two scenarios. Also, we will generate a database for simulations of various parameter settings. In this way, by comparing a disease curve from the real world with our database, we can tell which scenario the real world disease most closely resembles.

## **4.2 Future Research Topics**

We hope to explore the following research topics using our agent-based model:

- 1. Filter background noise**

Due to the influence of seasonal influenza, there will be background noise that affects the total number of infections reported by hospitals and clinics. Our goal will be to filter this background noise and distinguish between an epidemic and a bioterrorism disease.

- 2. Impact of multiple bioterrorism attacks**

We want to investigate how the execution of the bioterrorism attack will impact our detection ability. The biological agents can be released in a single or multiple locations in the same city, or multiple locations in different cities, so it is important to understand how the release pattern impacts disease recognition.

- 3. Impact of cities’ geographic and demographic traits**

By incorporating diverse geographic and demographic properties into the model (e.g., different city sizes, infection rates, travel patterns, etc.), we can examine how these differences impact our ability to determine whether a disease outbreak is due to a bioterrorism attack.

- 4. Early detection based on reports from individual cities**

Instead of examining the aggregate number of infected individuals in a region, we can investigate the transmission curve for each city. Is it possible to diagnose a bioterrorism threat in its early stage by looking at the infection number in each city?

- 5. Impact of the bioterrorism transition pattern**

Depending on the spreading pattern of the agent—whether it is transmitted by direct contact, air, contaminated water or food sources, or via vectors such as mosquitoes—we can investigate how each pattern will affect the transmission trend and further influence disease detection.

- 6. Impact of human behavior**

The public response may influence disease detection as well. On the one hand, patients may choose to stay home or go to a hospital, or to restrict social interaction. On the other hand, susceptible people may take medical prophylaxis such as antibiotics or vaccinations, or adopt physical protection such as gauze masks. All of these behaviors will impact the disease

infection curve and challenge our ability to distinguish the bioterrorism scenario from an epidemic.

7. **Impact of government policies**

We can investigate the influence of possible government policies for disease control such as quarantine or school closures.

8. **Suggestions to the Centers for Disease Control and Prevention and local health agencies**

By evaluating the effectiveness of various disease control approaches, we might provide suggestions on strategies or policies that should be adopted when facing a bioterrorism threat.

**APPENDIX**

If we assume a percentage of residents to be immune to the disease initially, then the infection curves will shrink by approximately that percentage in height. Figure 12 demonstrates the aggregated infection proportion under various immunity levels for bioterrorism and an extreme epidemic, respectively. In fact, if  $y$  represents the steady state aggregated infection percentage and  $x$  represents the immunity percentage, then the linear regression models for bioterrorism and an extreme epidemic disease are  $y = -0.33x + 0.3316$  ( $R^2 = 0.9609$ ) and  $y = -1.0512x + 0.94814$  ( $R^2 = 0.9965$ ). In both cases, increasing immunity by 1% reduces the height of the curve by 1% of the initial height (Since the initial height for the two diseases are 0.33 and 0.95, respectively).

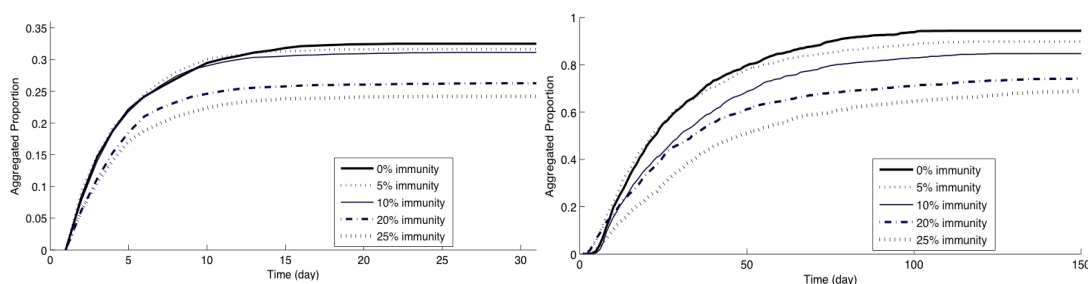


Figure 12: Aggregated infection proportion under various immunity levels for bioterrorism (left) and an extreme epidemic (right).

**REFERENCES**

Atkinson, W., J. Hamborsky, L. McIntyre, and S. Wolfe. 2005. *Epidemiology and Prevention of Vaccine-Preventable*. 9th ed. Washington DC: Public Health Foundation.

Bravata, D., J. Holty, H. Liu, K. McDonald, R. Olshen, and D. Owens. 2006. "Systematic review: a century of inhalational anthrax cases from 1900 to 2005." *Ann Intern Med* 144 (4): 270–280.

Clayton, D., M. Hills, and A. Pickles. 1993. *Statistical models in epidemiology*. 1st ed. Oxford: Oxford University Press.

CDC (Centers for Disease Control and Prevention) 2007. "Bioterrorism Overview." Last modified February 12<sup>th</sup>, 2007. <http://www.bt.cdc.gov/bioterrorism/overview.asp>.

CIDRAP (Center for Infectious Disease Research and Policy) 2013. "Tularemia: Current, comprehensive information on pathogenesis, microbiology, epidemiology, diagnosis, treatment, and prophylaxis." Last modified September 6<sup>th</sup>, 2013. [http://www.cidrap.umn.edu/infectious-disease-topics/tularemia -\\_Overview\\_1+CIDRAP&overview&1-2](http://www.cidrap.umn.edu/infectious-disease-topics/tularemia_-_Overview_1+CIDRAP&overview&1-2).

FAS (Federation of American Scientists) 2014. "Biological Threat Agents Information." Accessed April 10. <http://fas.org/programs/ssp/bio/resource/biothreatagents.html>.

Guillemin, J. 1999. *Anthrax: The Investigation of a Deadly Outbreak*. 1st ed. Oakland, California: University of California Press.

- Knobler, S., A. Mack, A. Mahmoud, and S. Lemon. 2005. *The Threat of Pandemic Influenza: Are We Ready? Workshop Summary*. 1st ed. Washington, D.C.: The National Academies Press.
- Lober, W., M. Wagner, A. Davidson, L. Trigg, and J. Espino. 2002. "Roundtable on bioterrorism detection: information system-based surveillance." *J Am Med Inform Assoc.* 9(2): 105-115.
- Mahaffy, J. M., and J. Dockery. 2013. "Influenza Modeling with a Discrete SIR model." Accessed July 1<sup>st</sup>, 2014. <http://www.math.montana.edu/~umsfjdoc/m430/Influenza.pdf>.
- Patterson, K., and G. Pyle. 1991. "The geography and mortality of the 1918 influenza pandemic." *Bull Hist Med.* 65 (1): 4–21.
- Roberts, F. S. 2003. "Challenges for Discrete Mathematics and Theoretical Computer Science in the Defense against Bioterrorism." In *Bioterrorism: Mathematical modeling applications in homeland security*, edited by Banks, H. T. and Castillo-Chavez, C., 1-34. Philadelphia, PA: SIAM.
- Taubenberger, J., and D. Morens. 2006. "1918 Influenza: the mother of all pandemics." *Emerg Infect Dis.* 12 (1): 15–22.
- Wagner, M., F. Tsui, J. Espino, V. Dato, D. Sittig, R. Caruana, L. McGinnis, D. Deerfield, M. Druzdzel, and D. Fridsma. 2001. "The emerging science of very early detection of disease outbreaks." *Public Health Management Practice* 7(6): 51-59.
- Wilensky, U. 1999. NetLogo. Center for Connected Learning and Computer-Based Modeling, Northwestern University, Evanston, IL. <http://ccl.northwestern.edu/netlogo/>.
- Yahav, I., S. Barnes, B. Golden, and E. Wasil. 2013. "Early Detection of Bioterrorism: Monitoring Disease Diffusion Through a Multilayered Network." In *Proceedings of the 2013 Industrial and Systems Engineering Research Conference*, edited by A. Krishnamurthy and W. K. V. Chan, 2561-2570. Norcross, Georgia: Institute of Industrial Engineers, Inc.

## **AUTHOR BIOGRAPHIES**

**SUMMER (XIA) HU** is a third year Ph.D. student in the Department of Mathematics (Applied Mathematics track) at the University of Maryland. Her current research interests are infectious disease modeling and simulation. Her email address is [xhu64@umd.edu](mailto:xhu64@umd.edu).

**SEAN BARNES** is an Assistant Professor of Operations Management in the Robert H. Smith School of Business at the University of Maryland, College Park. He holds his M.S. degree in Aerospace Engineering from Georgia Tech and Ph.D. degree in Applied Mathematics and Scientific Computing from the University of Maryland. His current research interests are modeling the transmission of infectious diseases, healthcare analytics, and simulation. His email address is [sbarnes@rhsmith.umd.edu](mailto:sbarnes@rhsmith.umd.edu).

**BRUCE GOLDEN** is the France-Merrick Chair in Management Science and a Full Professor in the Robert H. Smith School of Business the University of Maryland, College Park. He received his Ph.D. from M.I.T. in 1976. He served as Department Chairman of Management Science and Statistics from 1980 to 1996. His research interests include business logistics, networks, and healthcare analytics. He has won numerous awards including the Distinguished Scholar-Teacher Award, the INFORMS Computing Society Prize, and the Harvey J. Greenberg Award for lifetime contributions to the INFORMS Computing Society. He was named an INFORMS Fellow in 2004. Bruce has published extensively and is widely cited. He has served as the Editor-in-Chief of a major journal in his field since 1992. His email address is [bgolden@rhsmith.umd.edu](mailto:bgolden@rhsmith.umd.edu).